

Search for Contact Interactions in the Dimuon Final State at ATLAS

E. N. Thompson, S. Willocq
 University of Massachusetts, Amherst
 K. M. Black
 Harvard University

The Standard Model has been successful in describing many fundamental aspects of particle physics. However, there are some remaining puzzles that are not explained within the context of its present framework. We discuss the possibility to discover new physics in the ATLAS Detector via a four-fermion contact interaction, much in the same way Fermi first described Weak interactions. Using a simple ratio method on dimuon events, we can set a 95% C.L. lower limit on the effective scale $\Lambda = 7.5$ TeV (8.7 TeV) for the constructive Left-left Isoscalar Model of quark compositeness with $\mathcal{L} = 100$ pb $^{-1}$ (200 pb $^{-1}$) of data at $\sqrt{s} = 10$ TeV.

1. Introduction

New physics discovery may be just around the corner as the Large Hadron Collider (LHC) prepares for first collisions this winter. The Standard Model has thus far shown impressive predictive power and agreement with experiment; yet the cause of Electroweak Symmetry Breaking (EWSB), necessary to give mass to the W^\pm and Z^0 bosons, remains experimentally unconfirmed. In the last decades, many models outside of the current Standard Model framework have been developed to address this.

One way to model a new interaction with unknown couplings is in the form of a “4-fermion” contact interaction. Interactions with a dimuon final state have been chosen for this analysis, as they provide a clean signature in the early stages of understanding the ATLAS detector.

In the first year of LHC running, we expect 100 - 200 pb $^{-1}$ of data at $\sqrt{s} = 10$ TeV. In these proceedings, we discuss the feasibility of discovering or setting limits on new physics via contact interactions with early ATLAS data. Note also that the results presented here have not yet been officially approved by the ATLAS Collaboration.

2. Theoretical Background

Beyond the Standard Model processes, such as large extra spacial dimensions (LED) in the ADD model [1] or quark/lepton compositeness [2], may be described as a 4-fermion contact interaction. In the same spirit as the Fermi Interaction describes β -decay without directly knowing the intermediate process [3], one can write an effective Lagrangian describing a new interaction [4]:

$$\begin{aligned} \mathcal{L} = & \frac{g^2}{\Lambda^2} [\eta_{LL} (\bar{\Psi}_L \gamma^\mu \Psi_L) (\bar{\Psi}'_L \gamma_\mu \Psi'_L) \\ & + \eta_{RR} (\bar{\Psi}_R \gamma^\mu \Psi_R) (\bar{\Psi}'_R \gamma_\mu \Psi'_R) \\ & + \eta_{LR} (\bar{\Psi}_L \gamma^\mu \Psi_L) (\bar{\Psi}'_R \gamma_\mu \Psi'_R) \\ & + \eta_{RL} (\bar{\Psi}_R \gamma^\mu \Psi_R) (\bar{\Psi}'_L \gamma_\mu \Psi'_L)] , \end{aligned} \quad (1)$$

where g is a coupling constant, and $\Psi_{L,R}$ and $\Psi'_{L,R}$ are the incoming and outgoing left and right fermionic fields, re-

spectively. The interaction appears experimentally as a deviation from the SM dilepton mass spectrum, which originates from Drell-Yan (DY) production ($q\bar{q} \rightarrow \gamma, Z \rightarrow l^+ l^-$). The value of η is the sign of the interaction term; there can be either constructive ($\eta = -1$) or destructive ($\eta = +1$) interference with the DY process.

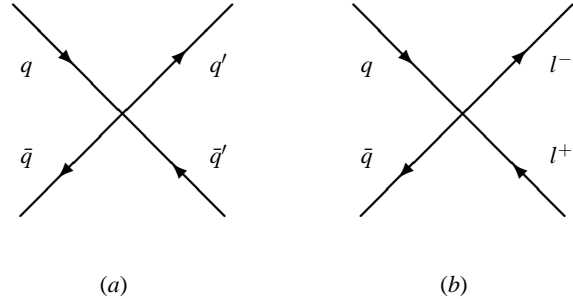


Figure 1: Representative Feynman diagrams for various 4-fermion contact interactions. Examples of possible production at the LHC are shown for (a) dijet production and (b) dilepton production.

Some examples of contact interaction diagrams are shown in Fig. 1. In the case of Fig. 1b, the “contact” can be understood as being between incoming partons and final-state charged leptons at some scale Λ . More specifically, the Lagrangian for the 4-fermion contact interaction with a dimuon final state ($qq\mu\mu$) is given by:

$$\begin{aligned} \mathcal{L} = & \frac{g^2}{\Lambda^2} [\eta_{LL} (\bar{q}_L \gamma^\mu q_L) (\bar{\mu}_L \gamma_\mu \mu_L) \\ & + \eta_{RR} (\bar{q}_R \gamma^\mu q_R) (\bar{\mu}_R \gamma_\mu \mu_R) \\ & + \eta_{LR} (\bar{q}_L \gamma^\mu q_L) (\bar{\mu}_R \gamma_\mu \mu_R) \\ & + \eta_{RL} (\bar{q}_R \gamma^\mu q_R) (\bar{\mu}_L \gamma_\mu \mu_L)] . \end{aligned} \quad (2)$$

Here, $q_{L,R}$ are the left- or right-handed quark doublets, $u_{L,R}$ and $d_{L,R}$ are the left or right quark singlets, and $\mu_{L,R}$ are the left- or right-handed muon singlets.

The total cross section is then given by the general form

$$\sigma = DY + \frac{I}{\Lambda^2} + \frac{C}{\Lambda^4} , \quad (3)$$

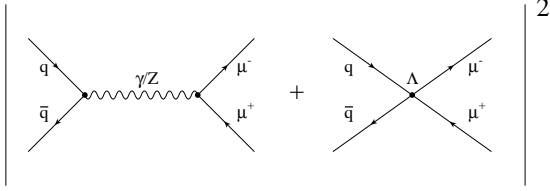


Figure 2: Production mechanism of Drell-Yan with additional contact term with scale Λ in the dimuon final state.

with a DY term (the cross-section of the Standard Model Drell-Yan spectrum), an interference term I which goes as Λ^{-2} , and the contribution of the contact interaction C which goes as Λ^{-4} .

3. Contact Interaction Analysis Method

Monte Carlo event generation using PYTHIA [5] has been done for the parity-conserving Left-left Isoscalar Model (L-LIM) of fermion compositeness, corresponding to the first term in Eq. (2). We chose four benchmark signal values to calculate the expected limit: $\Lambda = 5, 7, 9$ and 12 TeV. In the event generation stage, the following selection criteria were used:

- two or more final state muons from the hard scattering
- dimuon invariant mass $M_{\mu\mu} > 120$ GeV
- transverse momentum $p_T > 5$ GeV and pseudorapidity $|\eta| < 2.8$ for final state muons.

These requirements were chosen in order to increase statistics in the signal region and to be within the geometrical acceptance of the Muon Spectrometer. In Table I, we show the production cross-section times the muon branching fraction ($X \rightarrow \mu\mu$) for each of the benchmark Λ values. Detector response was simulated using the standard ATLAS fast simulation, and the resulting dimuon invariant mass was calculated. We then multiply by a mass dependent k-factor (ranging from 1.31 to 1.15 from 120 GeV to 2000 GeV [6]) and a dimuon reconstruction efficiency factor of $(0.85)^2 = 0.07225$. After event generation and fast simulation, muon candidates are chosen to be within pseudorapidity $|\eta| < 2.5$ (the geometrical acceptance of the Inner Detector [7]) and dimuons are required to have an invariant mass $M_{\mu\mu} > 120$ GeV. Fig. 3 shows the resulting dimuon differential cross-section in the constructive Left-left Isoscalar Model. The DY spectrum corresponds to $\Lambda \rightarrow \infty$.

3.1. Limit Setting and Discovery Potential Using the Ratio Method

One method to look for an excess of events in the high-mass DY spectrum is to simply count the number of events

Table I Cross-sections for benchmark Λ values in the constructive Left-left Isoscalar Model for pp collisions at $\sqrt{s} = 10$ TeV (for $M_{\mu\mu} > 120$ GeV).

Λ (TeV)	$\sigma \times bf$ [pb]
5	13.28
7	12.85
9	12.75
12	12.54
∞ (DY)	12.52

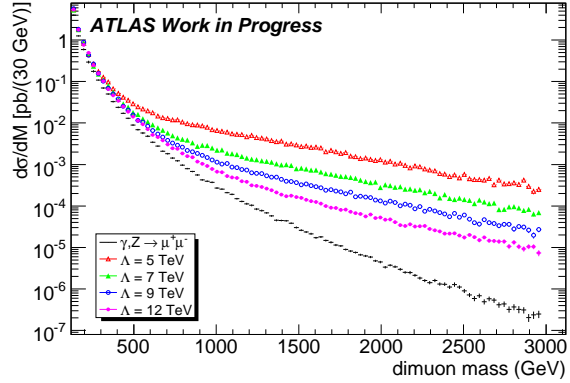


Figure 3: Dimuon invariant mass spectra for various Λ values. Note that the signal distribution tends to the DY shape as $\Lambda \rightarrow \infty$.

above an invariant mass threshold (M_0) and divide by the number of events in a control region where the expected shape and cross-section of the DY are tightly constrained from previous experiments:

$$R_{\Lambda, DY, d} = \frac{N_{M > M_0}}{N_{M < M_0}}. \quad (4)$$

Note that $R_{\Lambda \rightarrow \infty} = R_{DY}$, the expected ratio from the DY invariant mass spectrum. The number of events in any region is given by $N = \mathcal{L} \varepsilon \sigma bf(X \rightarrow \mu\mu)$, where \mathcal{L} is the integrated luminosity, ε is the acceptance and reconstruction efficiency, σ is the differential cross-section from Eq (3), and $(bf(X \rightarrow \mu\mu))$ is the branching fraction in the dimuon channel. When taking the ratio $R_{\Lambda, DY}$ from Monte Carlo simulations or R_d from collected data, the uncertainty in the luminosity cancels in the ratio. The effect of strongly-correlated uncertainties between the two regions is also reduced, which is especially advantageous in the first months of data taking, when the uncertainties are expected to be large.

The ratio in Eq. (4), expected for the DY-only spectrum, can be compared with an expected signal ratio using the following significance calculation:

$$S_{lim} = \frac{R_{\Lambda} - R_{DY}}{\sqrt{\sigma_{\Lambda}^2 + \sigma_{DY}^2}}. \quad (5)$$

Here σ_{Λ} is the statistical uncertainty on the signal ratio,

assuming that new physics did exist but had fluctuated downwards and was missed. Systematic uncertainties on the background ratio are incorporated in σ_{DY} , which include detector effects and our limited knowledge of Standard Model parton density functions, backgrounds, etc. In calculating the actual limit, we would use real data in place of the DY-only Monte Carlo sample for comparison to the ratio expected for a given Λ scale. The Λ scale which results in a significance of $S_{lim} = 1.96$ corresponds to a 95% confidence level limit.

3.2. Expected Reach With Early Data at $\sqrt{s} = 10$ TeV

The effect of systematic uncertainties on the significance calculation was determined for the DY background. It was found that muon resolution, muon efficiency, and k-factor uncertainties were the largest contributors to the overall ratio uncertainty, as they are momentum-dependent. The efficiency uncertainty was chosen to rise from 1% to 15% over the mass range of 120 GeV-2000 GeV, the resolution uncertainty calculation was based on a mis-alignment the Muon Spectrometer four times worse than design, and the k-factor uncertainty was based on minimizing and maximizing the slope of the mass-dependent k-factor functional form within errors previously determined [6]. Note that the values quoted are an exaggeration of expected first-year systematics. Table II summarizes these results.

Table II Expected systematics for the first months of ATLAS running. N_{high} and N_{low} are the expected number of events for 100 pb^{-1} above and below M_0 , respectively.

Mass cut @ 450 GeV	N_{low}	N_{high}	DY ratio	% diff
Nominal SM	660.5	7.6	0.0115	
Resolution	732.7	9.0	0.0123	6.7%
p_T scale (1% up)	699.3	7.9	0.0113	-1.5%
p_T scale (1% down)	632.5	7.3	0.0116	1.1%
Efficiency (up to 15%)	669.5	7.8	0.0117	2.0%
Efficiency (down 15%)	651.4	7.3	0.0112	-2.1%
k-factor (max slope)	635.3	7.4	0.0117	1.9%
k-factor (min slope)	700.5	7.8	0.0111	-3.1%

To determine the impact of statistical uncertainty in the signal ratios (σ_Λ), the RMS of R_Λ distributions from performing 10000 pseudo-experiments were calculated on each of the benchmark values (Fig. 4, Table III). The number of sample events (N_i) chosen for the i^{th} pseudo-experiment was determined from a Poisson distribution about the expected number of events $N_{expected}$ in 100 pb^{-1} (or 200 pb^{-1}) of data. Each pseudo-experiment was then created by randomly sampling N_i events from a dataset corresponding to hundreds of fb^{-1} .

The value of the expected ratios $R_{DY,\Lambda}$ are highly dependent on the choice of M_0 , the cutoff between the high and low dimuon invariant mass regimes. To account for this, we calculate S_{lim} as a function of M_0 (Fig. 5). The M_0

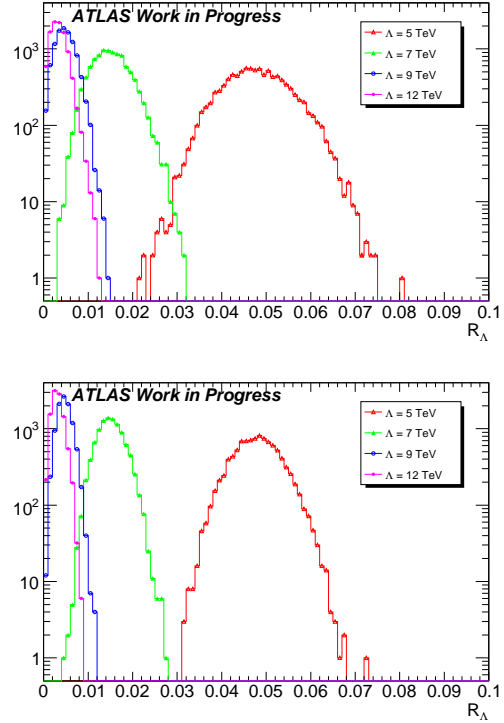


Figure 4: Comparing various R_Λ distributions for $\mathcal{L} = 100 \text{ pb}^{-1}$ (top) and 200 pb^{-1} (bottom).

which maximizes S_{lim} for each Λ value is used when setting the limit on Λ (see Table III). We have found that the maximum is very broad in M_0 , and that increasing the luminosity does not affect the chosen mass cut significantly.

Table III Ratios R_{DY} and R_Λ are shown for each Λ with corresponding best M_0 cut in 100 pb^{-1} .

Λ	Best M_0	Drell-Yan only		Drell-Yan + signal		
		$\frac{N_{high}}{N_{low}}$	R_{DY}	$\frac{N_{high}}{N_{low}}$	R_Λ	σ_Λ
5 TeV	450 GeV	10.20	0.0127	44.33	0.0541	0.0082
		805.52		820.95		
7 TeV	540 GeV	4.98	0.0062	13.66	0.0170	0.0046
		809.37		808.37		
9 TeV	750 GeV	1.27	0.0016	3.73	0.0046	0.0024
		812.36		820.56		
12 TeV	780 GeV	1.07	0.0013	2.00	0.0025	0.0017
		812.53		805.93		

Note that in early data, while the resolution uncertainty is the largest systematic, statistical uncertainty dominates in calculating the ratio (Fig. 6). After fitting the significance for the various Λ values (5, 7, 9 and 12 TeV), we expect to be able to set a new limit on the constructive L-LIS model of fermion compositeness at $\Lambda = 7.5$ TeV with 100 pb^{-1} , or $\Lambda = 8.7$ TeV with 200 pb^{-1} (Fig. 7).

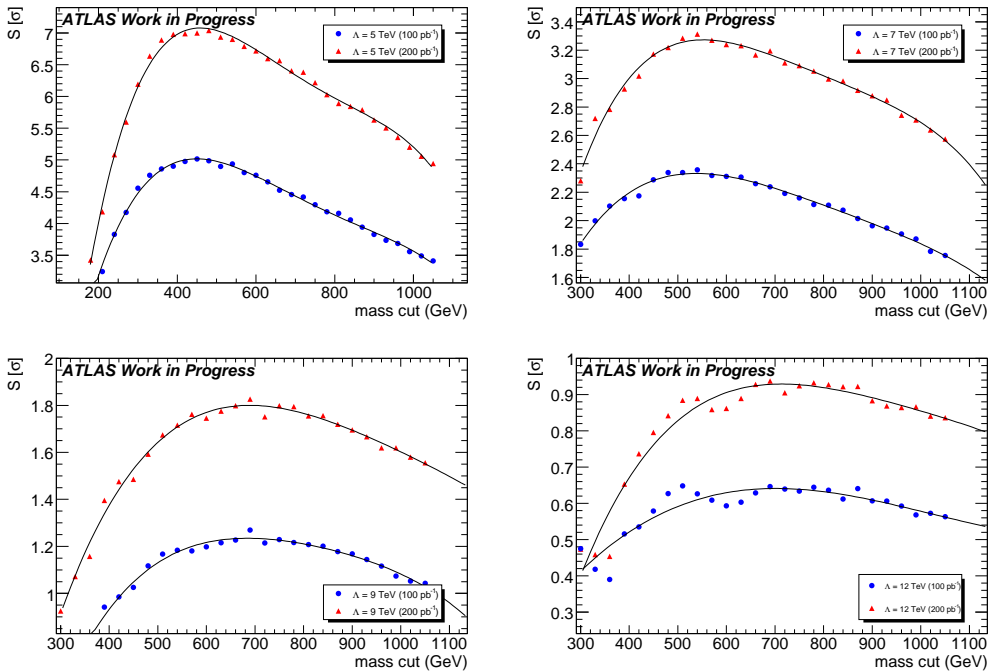


Figure 5: Distributions of significance (S_{lim}) by varying M_0 for different Λ values, with the blue curve corresponding to 100 pb^{-1} and the red curve corresponding to 200 pb^{-1} .

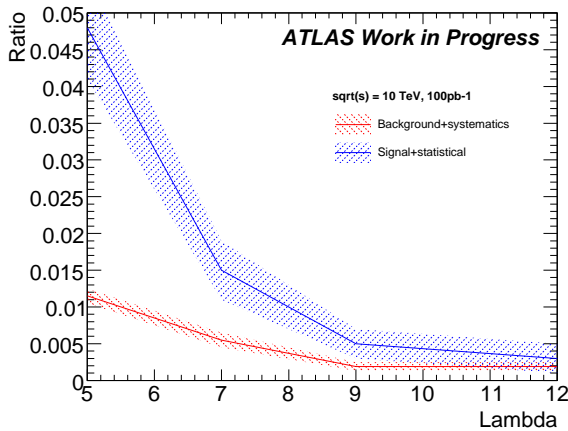


Figure 6: Ratio versus Lambda, using M_0 for maximized significance.

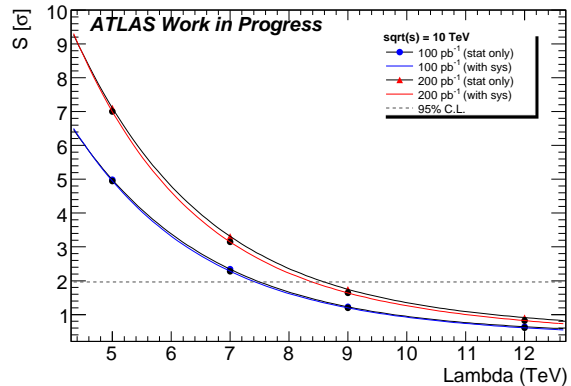


Figure 7: The expected 95% C.L. limit on Λ corresponds to a significance (S_{lim}) of 1.96σ , shown here for 100 pb^{-1} and 200 pb^{-1} .

References

- [1] N. Arkani-Hamed, S. Dimopoulos and G. Dvali, “The Hierarchy Problem and New Dimensions at a Millimeter”, *Physics Letters B* 429, doi:10.1016/S0370-2693(98)00466-3, 1998.
- [2] C. Amsler, et al. (Particle Data Group), *Physics Letters B* 667, 2008.
- [3] Tanikawa, Yasutaka, “Renormalizable Theory for Fermi Interactions”, *Phys. Rev.* 108 6, 1957.
- [4] E. Eichten, K. Lane, and M. Peskin, “New Tests for Quark and Lepton Substructure”, *Phys. Rev. Lett.* 50 11 811-814, 1983.
- [5] T. Sjöstrand, P. Edén, C. Friberg, L. Lönnblad, G. Miu, S. Mrenna and E. Norrbin, *Computer Phys. Commun.* 125 238 (LU TP 00-30, hep-ph/0010017, 2001.
- [6] ATLAS Collaboration, “Expected Performance of the ATLAS Experiment, Detector, Trigger and Physics”, CERN-OPEN-2008-020, 2008.
- [7] The ATLAS Collaboration, G. Aad et al., “The ATLAS Experiment at the CERN Large Hadron Collider”, *Journal of Instrumentation* 3 08 S08003, <http://stacks.iop.org/1748-0221/3/S08003>, 2008.